Colloidal Interactions and Self-Assembly Using DNA Hybridization

Paul L. Biancaniello,[1] Anthony J. Kim,[2] and John C. Crocker[2]

[1]*Department of Physics and Astronomy, University of Pennsylvania, Philadelphia, Pennsylvania 19104, USA*
[2]*Department of Chemical and Biomolecular Engineering, University of Pennsylvania, Philadelphia, Pennsylvania 19104, USA*
(Received 9 September 2004; published 10 February 2005)

The specific binding of complementary DNA strands has been suggested as an ideal method for directing the controlled self-assembly of microscopic objects. We report the first direct measurements of such DNA-induced interactions between colloidal microspheres, as well as the first colloidal crystals assembled using them. The interactions measured with our optical tweezer method can be modeled in detail by well-known statistical physics and chemistry, boding well for their application to directed self-assembly. The microspheres' binding dynamics, however, have a surprising power-law scaling that can significantly slow annealing and crystallization.

Much of the excitement regarding nanotechnology stems from the idea of "bottom-up" self-assembly: the possibility of spontaneously growing complex structures or devices out of molecular scale components rather than using conventional microfabrication. This goal requires a method for inducing specific interactions between multiple particle species and close attention to nucleation, growth, annealing, and thermodynamic stability. A leading contender for inducing such interactions is DNA hybridization, used to date for the self-assembly of quantum dots [1], colloidal microspheres [2,3], and assemblies themselves made from DNA [4]. Linking bridges of DNA can either glue two objects together strongly or cause them to weakly and reversibly adhere. While the strong adhesion limit has been studied [5], the weak reversible interactions required for equilibrium self-assembly and annealing remain poorly characterized, hindering experimental and theoretical progress. All previous attempts to assemble non-DNA objects using DNA interactions have created highly disordered aggregates rather than the hoped for crystal-like structures.

Here we report direct measurements of the equilibrium, DNA-induced interaction potential and adhesion dynamics of pairs of polymer microspheres. The interaction's range and strength can be modeled in detail using a simple statistical mechanics framework and well-known chemical parameters [6]. The microsphere dynamics, however, show an anomalous power-law binding lifetime distribution that slows crystal nucleation and growth. We find that combining a modest surface density of DNA with a sterically stable colloidal surface enables the growth of small colloidal crystals in ~50 h. While highlighting the experimental challenges, our work provides a foundation for the quantitative design and modeling [7] of directed self-assembly processes.

Figure 1 shows our system, consisting of 0.98 μm diameter polystyrene microspheres, each labeled with identical DNA oligonucleotides. The ends of these DNA strands can be bridged together via the reversible hybridization of "linker" strands in solution [Figs. 1(b) and 1(c),

shaded boxes], inducing a short-ranged attraction between microspheres. DNA thermodynamic models [6] predict that these bridges become unstable above ~47 °C [Fig. 2(c)]. The hybridizable ends are separated from the microsphere surface by a spacer consisting of either flexible [8] single-stranded DNA or rigid [9] double-stranded DNA, which sets the range of the interaction. All DNA sequences were designed to have low secondary structure and minimal sequence repetition with melting temperatures for all nondesigned conformations below 25 °C. The colloidal surfaces are either carboxylate-modified polystyrene latex (CML) [2] or polyethylene glycol (PEG) [10] grafted polystyrene; the oligonucleotides are
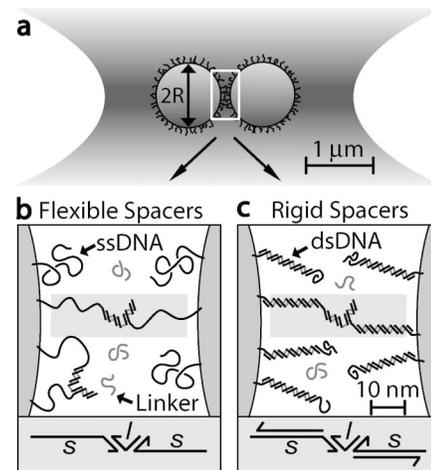

FIG. 1.   (a) represents two microspheres trapped in the focal plane of a line optical tweezer. (b) shows microsphere surfaces chemically grafted with oligonucleotides, *s*, (sequence: <u>ACTTAACTACAGCATTATCAGTCTCCGAGGCCCATTG-ATTCACACACGTCT</u>**AACTTGAAATCTCT**). Linker oligonucleotides, *l*, (sequence: AGAGATTTCAAGTTCAGAGATTT-CAAGTT) can bridge between microspheres (shaded boxes) after hybridizing with the terminal 14 bases of *s* (bold sequence). (c) same as (b) after hybridization of a third oligonucleotide complementary to *s* (underlined sequence), forming a rigid rodlike spacer.

covalently linked to these polymers via a $5'$-amine modification. Tween-20 was added (0.1%) to the aqueous buffer (10 mM Tris, *p*H 8.0, 100 mM NaCl) to stabilize the CML samples. While many studies use mixtures of microspheres bearing dissimilar DNA sequences [1–3], we use a one-component system for its better understood self-assembly behavior.

We directly measured the DNA-induced microsphere pair interaction and dynamics using a continuous wave line optical tweezer [11] [Fig. 1(a)] and video microscopy [12] using a high-speed camera (Phantom 4.0, Vision Research, Inc.). Stretching an ordinary optical tweezer ($\sim$100 mW, $\lambda = 830$ nm; Melles-Griot) into a line focus using a Keplerian cylindrical telescope creates a nearly harmonic potential for two microspheres along the line, while strongly confining them in the perpendicular directions. Light from a second, pulsed multimode diode laser (2 W, $\lambda = 808$ nm, Spectra Diode Labs) provides illumination, yielding exposure times <40 μs. The equilibrium pair interaction is computed from the probability distribution of their separation via the Boltzmann relation, corrected for optical forces [11]. Figure 2 displays the measured interaction potential energy between pairs of DNA-grafted CML microspheres as a function of temperature with either flexible or rigid spacers. The data indicate a
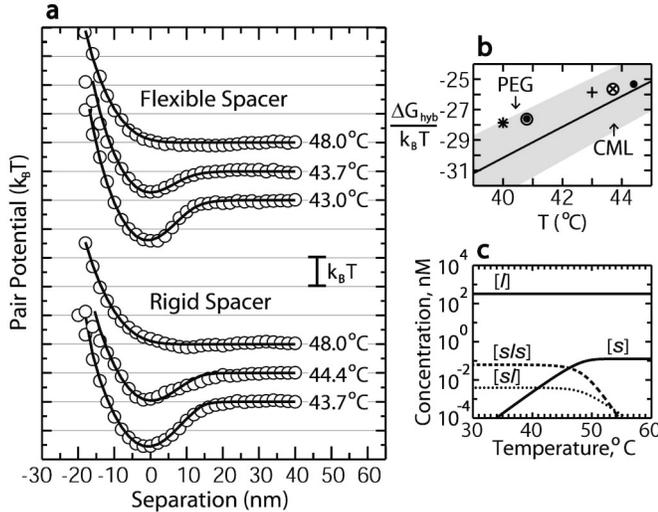

FIG. 2. (a) Pair potential energy between two DNA-grafted microspheres as a function of separation, temperature, and spacer. The flexible spacer data, as in Fig. 1(b), is at the top (circles). The rigid spacer data, as in Fig. 1(c), is at the bottom (circles); it has a longer range and is stronger at a given temperature. Curves show our single parameter model, numerically blurred to account for instrumental resolution. Separation here is defined relative to the potential minimum. (b) shows the best fit values of hybridization free energy, $\Delta G_{\text{hyb}}(T)$, for the flexible ($\bigcirc$, $+$) and rigid ($\bullet$, $\times$) spacers, with *a priori* prediction (line) with $2.5 k_B T$ expected standard error (shaded region). (c) Bridge formation can be modeled as two coupled hybridization reactions: $s + l \leftrightarrow sl$ and $sl + s \leftrightarrow sls$. Approximate melting curves for these DNA structures are shown.

short-range attraction that decreases in strength as the temperature increases, vanishing by 48 °C, along with a soft, temperature independent repulsion near contact.

We model the pair interaction in our system as an attraction due to dynamically forming and breaking DNA bridges between the microspheres, acting as entropic springs, and an entropic repulsion due to compression of the grafted DNA. For sphere separation h and polymer spacer length L, the attraction has range $h < 2L$. DNA on one sphere colliding with the opposing sphere produces a repulsion with range $h < L$ (DNA density is low enough, $\sim 10^4$ strands per microsphere or less, that we can neglect DNA-DNA collisions). While the enthalpy of hybridization presumably generates a transient force during helix formation [5], we neglect its contribution to the time-averaged interaction.

The attractive interaction is an equilibrium average over many states with one or more ligand-receptor bridges. It can be easily computed if each of the N ligands has the same, statistically independent probability, p, of forming a bridge. The probability no bridges form is then $P_{\text{free}} = (1 - p)^N$ and the probability one or more bridges form is $P_{\text{bound}} = 1 - P_{\text{free}}$. The difference in Helmholtz free energy is

$$\frac{\Delta F_a}{k_B T} = -\ln\left(1 + \frac{P_{\text{bound}}}{P_{\text{free}}}\right) = N\ln(1 - p) \approx -Np = -\langle n \rangle,$$
(1)

for $p \ll 1$. Remarkably, the interaction energy is simply $k_B T$ multiplied by the number of bridges that form in chemical equilibrium at a given separation, $\langle n \rangle$. Since our DNA density permits about 50 strands to span between spheres in contact, only a few percent of the available strands need hybridize to induce the weak attraction seen in Fig. 2.

We first compute the total interaction, repulsive and attractive, between flat plates due to the grafted DNA and then convert it to the two sphere geometry using the Derjaguin approximation. If $P_h(x)$ is the probability distribution of the height of the grafted polymer, the entropic repulsion is [13]

$$\frac{\Delta F_r}{k_B T} = -\ln[\Omega(h)/\Omega(\infty)] \approx -\ln\int_0^h P_h(x)dx, \quad (2)$$

where Ω is the number of polymer states and the approximation is valid at long range. Computing the attraction using Eq. (1) requires the use of a mass-action law generalized for spatially nonuniform reacting ligand species [14]. We assume the mean ligand concentration, $P_s(x)$, depends only on the distance from the plate surface, x. The attraction per unit area between plates is

$$\frac{\Delta F_a}{A} \approx -k_B T c_l \sigma_s^2 \frac{e^{-\Delta G/k_B T}}{c_o^2} \frac{\int_0^h P_s(x)P_s(x - h)dx}{[\int_0^h P_s(x)dx]^2}, \quad (3)$$

where c_l is the concentration of linker oligonucleotide, σ_s is the areal number density of s strands, $c_o = 1$ M is a

reference concentration, and ΔG is the total change in Gibbs free energy to form a single DNA bridge; it includes both the hybridization free energy ΔG_{hyb} of the DNA and changes in the spheres' rotational entropy, $\Delta S_{rot} = k_B \ln(\langle \Theta_b / \Theta_f \rangle)$, due to bridge linking. Θ_b is the equilibrium averaged solid angle accessible to the bridged spheres, computed using the wormlike chain model [15] and Θ_f is the unbridged solid angle. Equation (3) indicates the interaction potential energy is proportional to the overlap of ligand clouds surrounding particles or surfaces, reminiscent of the well-known depletion interaction [16,17].

To compute the pair interaction, we used the geometric parameters of DNA [8,9] to model the DNA spacer conformation, described by $P_h(x)$ and $P_s(x)$, then evaluated Eqs. (2) and (3) using analytical and numerical methods. DNA content was measured by flow cytometry and UV spectrophotometry. We treated the flexible spacers as tethered Gaussian coils [13] with moments determined by a simple random walk simulation. The rigid spacers were modeled as tethered rigid rods [18], shortened by thermal undulations [19], having uniform probability distributions [17]. Spacer contour lengths [20] include a seven base length correction to account for the linker segment [Figs. 1(b) and 1(c)]; this was assumed to be single stranded in computing the repulsion, $P_h(x)$, and double stranded for the attraction, $P_s(x)$; otherwise the probability distributions would be identical. For comparison with data, the model potentials were numerically blurred to account for instrumental resolution ($\Delta h_{rms} \approx 5$ nm, determined by control measurements).

We performed a least-squares fit of the interaction model using total bridge formation energy $\Delta G(T) = \Delta G_{hyb}(T) - T\Delta S_{rot}$ as a free parameter, along with a horizontal shift to account for microsphere diameter variation. These values were then corrected using computed values of $T\Delta S_{rot} \approx -6k_B T$ for a single DNA bridge. The resulting ΔG_{hyb} were then compared with the nearest-neighbor model [6] (Fig. 2 inset). Overall, model agreement is excellent: ΔG_{hyb} for the four cases (flexible and rigid spacer, PEG and CML substrate) with weak sphere attractions (circle symbols) mutually agree with a $0.6k_B T$ standard deviation. Their mean differs from the *a priori* prediction by only $1.1k_B T$, well within the $2.5k_B T$ error expected for the nearest-neighbor model. The corresponding four cases with stronger sphere attractions (cross symbols) show an unphysical decrease in their mean ΔG_{hyb} of about $1k_B T$, which could likely be rectified with a more detailed calculation of rotational entropy effects. Nevertheless, our model predicts the interaction *a priori* with remarkable accuracy: $1k_B T$ of error in ΔG_{hyb} corresponds to only a ~ 1 °C shift in interaction temperature dependence.

Curiously, the CML colloid samples failed to crystallize after several days under favorable conditions [21]: $1 - 4k_B T$ pair attraction and volume fraction $> 20\%$. Instead, the lower temperature samples formed fractal-like aggre-

gates [3] over the course of several hours [Fig. 3(a)]. These structures dissociated upon heating by a few degrees, presumably ruling out inadequate colloidal stability as the explanation. However, trace amounts of irreversibly bond dimers and trimers were present in the CML samples, suggesting that some nonspecific binding did occur. We hypothesized that the slow dynamics were due to lubrication forces in the polymer-filled gap between the spheres, and could be sped up by reducing the DNA density. Lower DNA density, however, requires a PEG-ylated surface to produce sufficient colloidal stability against irreversible aggregation. PEG-based microspheres grafted with a low density of DNA (3700 DNA/sphere vs 14 000 DNA/sphere for CML) did successfully crystallize within 48 h, yielding small crystallites that grew to ~ 1000 spheres/crystal after 96 h [Figs. 3(b) and 3(c)]. While detailed crystallography is difficult using optical microscopy, the crystallites resembled homogeneously nucleated random hexagonal close-packed crystals formed using the depletion interaction. Identical samples incubated simultaneously 0.6 °C warmer and cooler remained dispersed or formed aggregates, respectively. Crystals melted immediately when the temperature was raised by 2 °C, confirming that they were formed and held together by DNA bridges [Fig. 3(d)].

To study the binding dynamics in detail, we examined the time-varying separation between two DNA-grafted microspheres in our trap [Fig. 4(a)]. The microspheres are alternately bound by DNA bridges ($h < 2L$) or un-
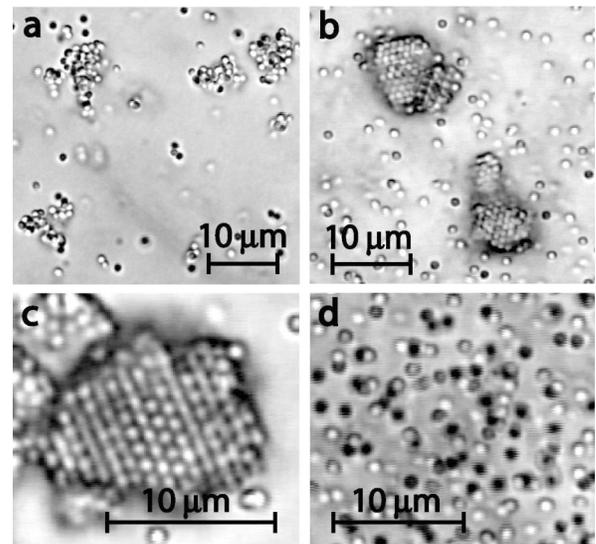

FIG. 3. Optical micrographs of colloidal microspheres assembled by DNA hybridization. (a) Colloidal spheres with $\sim 14\,000$ DNA/sphere on a CML surface formed only fractal-like aggregates after 96 h. (b) Similar spheres with ~ 3700 DNA/sphere on a PEG surface formed crystallites, shown after 96 h of growth. (c) A close-up of the front surface of one of the crystallites. (d) All crystallites and aggregates melted immediately upon heating by 2 °C, confirming they are held together by DNA bridges.
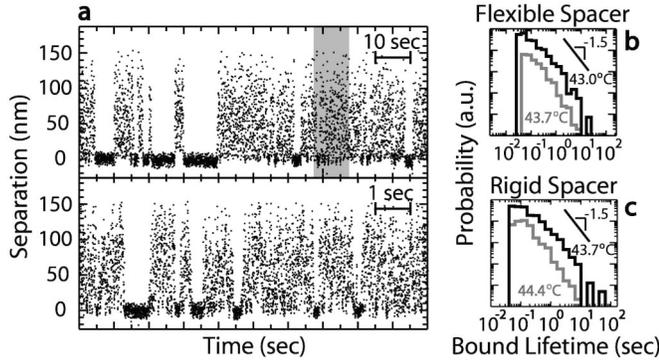
FIG. 4. (a) shows the separation distance vs time for two DNA-grafted microspheres in a line optical tweezer, for 100 sec (top) and 10 sec (bottom and shaded box); flexible spacer, $T = 43.0\,^{\circ}$C. The microspheres are alternately binding and unbinding, with a very broad distribution of bound lifetime. (b) and (c) show double logarithmic probability distributions of binding lifetime for the flexible and rigid spacer systems, respectively. The distributions have an anomalous power-law tail, with exponent roughly -1.5.

bound and diffusing to the width of the optical trap. The expected lifetime of the DNA bridges and the microspheres' diffusive escape time are both ~ 10 ms. While a subset of bound states are that short-lived, many other bound states last up to tens of seconds. These long-lived events have a power-law distribution $P(t) \sim t^b$ which gives rise to the self-similar appearance of the separation trajectories [Fig. 4(a)]. We observe $b \approx -1.5$ for both spacer types and temperatures [Figs. 4(b) and 4(c)]. Remarkably, the PEG-ylated spheres with lower DNA density show very similar dynamics, suggesting power-law kinetics are not incompatible with crystallization. While such slow binding dynamics can account for earlier failures to produce colloidal crystals, the relative contribution of DNA density, PEG-ylation, and nonspecific binding on crystallization remains an open question.

Directed self-assembly using these potentials should conform to existing theories for nucleation, growth, and annealing. Future theoretical work can use such model potentials with confidence to determine optimal self-assembly strategies for novel equilibrium structures, such as colloidal alloys [7] with potential photonic or plasmonic activity. Nucleating complex or large ordered structures may require the use of a microfabricated template [22]. The curvature dependence of the particle-surface potential corresponding to Eq. (2) should permit the use of a simple microcorrugated template [23].

Our results show that polymer spaced reacting ligands give rise to a readily predictable interaction in the weak adhesion limit, with strength set by the ligands' solution thermodynamics and spatial form determined by the spacer conformation [7]. Our experimental approach and theoretical framework should also be useful for understanding weak adhesion mediated by biological ligand-receptor pairs. Given that the slow dynamics we observe will likely improve as particle size is reduced below the micron scale, there appears no barrier to the programmed self-assembly of complex ordered structures using DNA.

[1] C. A. Mirkin, R. L. Letsinger, R. C. Mucic, and J. J. Storhoff, Nature (London) **382**, 607 (1996).
[2] C. M. Soto, A. Srinivasan, and B. R. Ratna, J. Am. Chem. Soc. **124**, 8508 (2002).
[3] V. T. Milam et al., Langmuir **19**, 10 317 (2003).
[4] N. C. Seeman, Nature (London) **421**, 427 (2003).
[5] G. U. Lee, L. A. Chrisey, and R. J. Colton, Science **266**, 771 (1994).
[6] J. J. SantaLucia, Proc. Natl. Acad. Sci. U.S.A. **95**, 1460 (1998).
[7] A. V. Tkachenko, Phys. Rev. Lett. **89**, 148303 (2002).
[8] M. C. Murphy et al., Biophys. J. **86**, 2530 (2004).
[9] P. J. Hagerman, Annu. Rev. Biophys. Biophys. Chem. **17**, 265 (1988).
[10] C. Monfardini et al., Bioconjugate Chem. **6**, 62 (1995).
[11] J. C. Crocker, J. A. Matteo, A. D. Dinsmore, and A. G. Yodh, Phys. Rev. Lett. **82**, 4352 (1999).
[12] J. C. Crocker and D. G. Grier, J. Colloid Interface Sci. **179**, 298 (1996).
[13] A. K. Dolan and S. F. Edwards, Proc. R. Soc. London A **337**, 509 (1974).
[14] A. K. Dutt and A. Datta, J. Phys. Chem. A **102**, 7981 (1998).
[15] C. Bustamante, J. F. Marko, E. D. Siggia, and S. Smith, Science **265**, 1599 (1994).
[16] S. Asakura and F. Oosawa, J. Polym. Sci. **33**, 183 (1958).
[17] The attractive interaction for the rigid case is

$$\frac{\Delta F_a}{k_B T} = -c_l \sigma_s^2 \frac{e^{(-\Delta G / k_B T)}}{c_o^2} \frac{\pi R}{2L^2} (h - 2L)^2,$$
$$L < h < 2L.$$

[18] E. L. Mackor, J. Colloid Sci. **6**, 492 (1951).
[19] O. Kratky and G. Porod, Recl. Trav. Chim. **68**, 1106 (1949).
[20] For the flexible case, simulations gave first and second moments of $m_1 = 6.11$ nm and $m_2 = 6.29$ nm for the attractive part and $m_1 = 6.70$ nm and $m_2 = 6.66$ nm for the repulsive part. For the rigid case, the "top hat" distribution has width $L = 18.20$ nm for the attractive part and $L = 20.20$ nm for the repulsive part.
[21] A. G. Yodh et al., Philos. Trans. R. Soc. London A **359**, 921 (2001).
[22] A. VanBlaaderen, R. Ruel, and P. Wiltzius, Nature (London) **385**, 321 (1997).
[23] K. H. Lin et al., Phys. Rev. Lett. **85**, 1770 (2000).